Adsorption of Chloroform in NaY Zeolite: A Computational and Vibrational Spectroscopy Study

Caroline F. Mellot,[†,‡] Anne M. Davidson,[†,§] Juergen Eckert,[||] and Anthony K. Cheetham*[,†,‡]

Materials Research Laboratory, University of California, Santa Barbara, California 93106, and Los Alamos National Laboratory, Los Alamos, New Mexico 87545

Received: October 31, 1997; In Final Form: January 27, 1998

The structure and energetics of chloroform binding sites in NaY zeolite have been studied by energy-minimization calculations and vibrational spectroscopy. A new force field for chlorocarbon-type molecules in zeolites has been developed. Our simulations predict the adsorption of chloroform in the 12-ring window where the hydrogen atom is involved in a hydrogen bond with the framework oxygens. This interaction is clearly revealed by inelastic neutron scattering and Raman spectroscopies, which show a typical softening of the stretching mode (ν_1) and a hardening of the bending mode (ν_4) involving the H atom of the adsorbed chloroform molecule. The overall host−guest interaction energy involves three components that have been identified as being typical of hydrohalocarbon adsorption in zeolites: (i) short-range interactions between chlorine and framework oxygens, (ii) electrostatic interactions between chlorine atoms and accessible Na ions, and (iii) hydrogen bonding with the framework oxygens.

Introduction

An increased awareness of environmental issues relating to ozone-depleting chlorofluorocarbons (CFCs)[1] and to the removal of chlorinated solvent residues from contaminated groundwater and soils[2] is driving the need to develop new separation and catalytic conversion processes for halocarbons. Zeolites have recently been recognized as interesting alternatives to other separation media such as activated carbons. For example, zeolite A and the naturally occuring clinoptilolite are efficient for the recovery of methyl chloride from the vent streams generated during the direct synthesis of methylchlorosilane.[3] Similarly, the basic NaX and NaY faujasites can be used to separate various hydrofluorocarbons during the manufacture of CFC substitutes.[4] In another context, the hydrophobic silicalite (siliceous ZSM-5) is a good candidate for the sequestration of chloroethylenes from groundwater.[5,6] As a consequence, a need is emerging for developing a better understanding of halocarbon adsorption in zeolites at a molecular level.

Unlike the situation with hydrocarbons, few experimental data concerning the adsorption of halocarbons in zeolites and analogous microporous materials have been reported so far. The heats of adsorption of several chlorofluorocarbons in deuterated Y zeolite have been estimated by calorimetric methods.[7] Isotherm measurements from the gas phase have been reported for a limited number of adsorbate/zeolite systems: dichlorodifluoromethane in Na−, K−, and Cs−Y zeolites,[8] chloroform in dealuminated faujasites,[9] tetrachloroethylene in dealuminated Y and ZSM-5.[6] IR and NMR spectroscopies have also been used to examine the behavior of carbon tetrachloride in various zeolites, exploring the role of this adsorbate in framework dealumination[10] and its co-adsorption with xenon to examine the interplay between a ^{129}Xe NMR probe and the CCl_4 molecules.[11] In the context of the catalytic conversion of halocarbons, the influence of the basicity of the framework oxygens of NaX and NaY zeolites on the chemical reactivity of methyl halides has been discussed.[12−15] The chemisorption of halocarbons in zeolites has recently been investigated by FTIR spectroscopy, including a new method for characterizing the zeolite basicity from chloroform adsorption[16] and a study of chloroethylenes in Cr−Y zeolite.[17] As far as the structures of simple halocarbons in zeolites are concerned, various simple halocarbons have been located in zeolites using an analysis of X-ray powder diffractograms by the Rietveld method: methyl chloride in zeolite rho[18] and chlororoform,[19] dibromobutane,[20] and CHF_2CHF_2[21] in NaY. While these studies yielded relevant models for the locations of the halocarbons, both the accuracy and the completeness of the sorption site geometries were limited by the low X-ray scattering factors of carbon and hydrogen atoms and, even more so, by the difficulty of dealing with highly disordered sorption sites.

In view of the growing interest in the adsorption of halocarbons in zeolites, we have undertaken a program aimed at developing reliable computer-simulation procedures that can be used to complement and enhance the analysis of experimental data (thermodynamic as well as spectroscopic and structural measurements). A preliminary study dealing with the adsorption of several CFCs and HCFCs in siliceous zeolites has been recently reported.[22] The present work focuses on the behavior of chloroform in the NaY zeolite, which can be considered as a model for chlorocarbon/zeolite systems. A previous synchrotron diffraction study[19] indicates that, in NaY zeolite, the chloroform molecules are physically adsorbed on the zeolitic walls, with their hydrogens pointing toward the center of the supercage (Figure 1a). We have used a combination of packing and energy-minimization calculations to probe the host−guest

* Corresponding author. E-mail: cheetham@mrl.ucsb.edu.
† University of California.
‡ Present address: Institut Lavoisier, UMR CNRS 173, Université de Versailles Saint-Quentin, 45 avenue des Etats-Unis, 78035 Versailles cedex, France.
§ Present address: Laboratoire de Réactivité de Surface, URA 1106-CNRS, 4 place Jussieu, 75252 Paris cedex 05, France.
|| Los Alamos National Laboratory.

S1089-5647(98)00042-X CCC: $15.00
Published on Web 03/17/1998

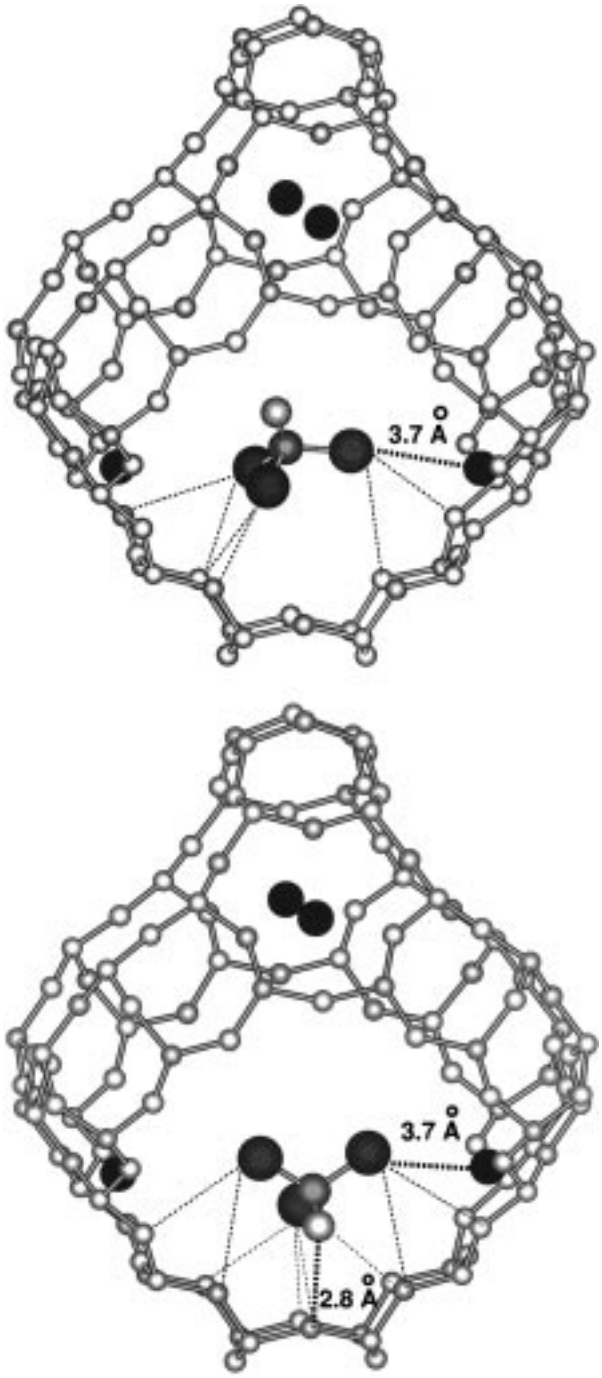

Figure 1. Binding geometry of chloroform adsorbed in NaY from (a, top) previous X-ray powder diffraction work[19] and (b, bottom) our computer simulations. In both cases, the Cl···O distances range typically from 3.5 to 3.8 Å.

potential energy surface and to confirm the sorbate location. Our force-field calculations are supported by two complementary spectroscopic studies. First, we have used inelastic neutron scattering (INS) to study the specific role of the C−H bond in the adsorption behavior of chloroform at low coverage (less than 1 molecule per supercage) and at low temperature (10 K). Second, chloroform adsorption has been followed by in-situ Raman spectroscopy at room temperature.

Computational and Experimental Methodologies

Docking of Chloroform in NaY. The so-called Monte Carlo packing procedure[23] was used to investigate the binding sites of chloroform in NaY zeolite in terms of site geometries and interaction energies. Calculations were carried out in a fashion similar to those reported in ref 24. A model structure for NaY, $Na_{48}Al_{48}Si_{144}O_{384}$, was built by using the atomic coordinates reported in ref 19 and placing the 48 cations in sites I and II.

The total host−guest interaction energy was taken as the sum of a short-range term, modeled with a (6−12) Lennard-Jones potential, and a long-range Coulombic term:

$$E_{\text{Lennard-Jones}} = \sum_{ij}(A_{ij}/r^{12} - B_{ij}/r^{6}) = \sum_{ij}\epsilon_{ij}\,[(r^{*}_{ij}/r_{ij})^{12} - 2\,(r^{*}_{ij}/r_{ij})^{6}] \quad (1)$$

$$E_{\text{Coulombic}} = \sum_{ij} q_i q_j / r_{ij} \quad (2)$$

where A_{ij} is the repulsive constant and B_{ij} the dispersive constant, with $\epsilon_{ij} = B^2_{ij}/4A_{ij}$, $r^{*}_{ij} = (2A_{ij}/B_{ij})^{1/6}$. The host−guest induction energy was neglected; a recent study[25] using elaborate intermolecular potential functions for simulating the adsorption of rare gases (Ar, Xe) in zeolites confirms the validity of this assumption. In these systems, the contribution of the induction term is estimated to be less than 0.3% of the total potential energy.

The short-range contribution of the zeolite host was calculated only using framework oxygens and Na cations; the contribution of Si and Al atoms was neglected since they have lower polarizabilities than oxygens and cannot be approached closely by sorbate molecules. The $CHCl_3$ molecule was described by a five-site model. Short-range parameters between $(C, H)_{\text{chloroform}}$ atoms and $(O, Na)_{\text{zeolite}}$ atoms were taken from Monte Carlo simulation studies that reported good predictions of experimental adsorption heats of methane in various zeolites: faujasite, mordenite, and ZSM-5.[26,27] Short-range parameters between $Cl_{\text{chloroform}}$ atoms and $(O, Na)_{\text{zeolite}}$ atoms were derived from those of argon in zeolitic structures. This was believed to be a reasonable approach since Ar and Cl have similar atomic radii (∼0.99 Å) and polarizabilities (1.64×10^{-24} cm^3 and 2.18×10^{-24} cm^3, respectively). The $\epsilon_{\text{Cl}\cdots\text{O}}$ parameter was derived from the $\epsilon_{\text{Ar}\cdots\text{O}}$ parameter used for simulating the adsorption of Ar in silicalite,[28] applying a first increase in a ratio of 1.1:1 accounting for the increase in the polarizability of in-framework oxygens from silicalite to NaY,[29] and a second increase in a ratio of 1.33:1 to take into account the change in polarizability from Ar to Cl. For determining short-range interactions between Cl and Na cations, preliminary (*N, V, T*) Monte Carlo simulations were carried out on Ar in NaX, with the aim of adjusting the $\epsilon_{\text{Ar}\cdots\text{Na}}$ parameter to reproduce the experimental heat of adsorption of Ar in NaX (Si:Al = 1.25) at 298 K. Working with our model structure for NaLSX (Si:Al = 1)[30] and using the following parameters, $\epsilon_{\text{Ar}\cdots\text{O}} = 160$ K and $r^{*}_{\text{Ar}\cdots\text{O}} = 3.43$ Å, close agreement between the simulated (−10.8 kJ/mol) and experimental (−11.7 kJ/mol)[31] heats of adsorption was obtained. Finally, the $\epsilon_{\text{Cl}\cdots\text{Na}}$ parameter was deduced by increasing the $\epsilon_{\text{Ar}\cdots\text{Na}}$ parameter by a factor of 1.33, as before.

The zeolite structure was kept rigid and considered as semi-ionic using partial charges that are consistent with those in ab initio silicate potentials[32] and recent X-ray diffraction results.[33] For circumventing the difficulty of the disordered distribution of Al atoms in the framework, an average T-atom (Al, Si) was considered and its charge chosen to satisfy a Si:Al ratio of 3. Charges for chloroform were derived from a Hartree−Fock calculation (TURBOMOLE)[34] using a 6-31G** basis-set and fitting the electrostatic surface potential. However, an overestimation of 20% of the dipole moment was found when compared to its experimental value of 1.06 D, so a single scale

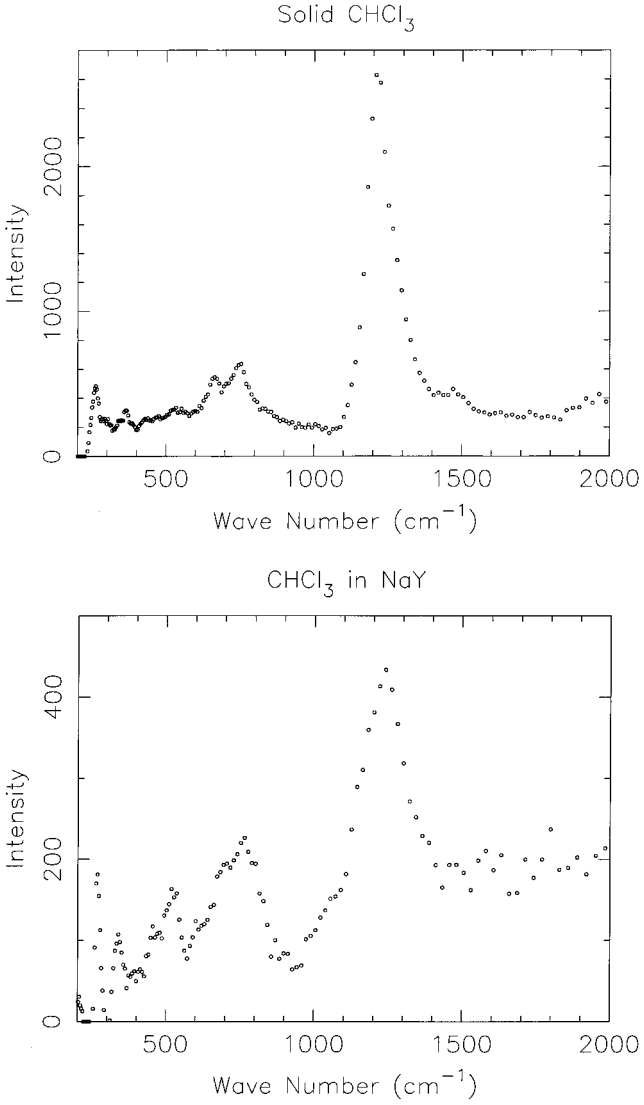

Figure 2. Inelastic neutron scattering spectra at low temperatures of (a, top) solid chloroform and (b, bottom) chloroform adsorbed in zeolite NaY at low loading (~1 molecule/supercage).

factor was applied to the above charges in order to reduce the dipole moment to the correct value.

Table 1 gives the short- and long-range parameters used in this work. All calculations were carried out using DIZZY[35] with a short-range summation taken up to a cutoff radius of 12 Å and an Ewald summation for the electrostatic term.

Inelastic Neutron Scattering and Raman Spectroscopy. The INS spectrum of 5 g of NaY (Si/Al = 2.6), after dehydration at 800 K, was collected at $T = 25$ K using a closed-cycle He refrigerator on the FDS instrument[36] at the Manuel Lujan Jr. Neutron Scattering Center of Los Alamos National Laboratory. The INS spectrum of the parent material loaded with one chloroform molecule per supercage was then measured under similar conditions. A spectrum was also recorded at 15 K on solid chloroform for comparison. These spectra were analyzed after background subtraction by deconvolution of the instrumental response function.[37]

The Raman spectra were collected at room temperature on a NIR-FT Raman Nicolet 850 spectrometer using an excitation laser with a wavelength of 1064 nm, at low power (typically less than 0.5 W on the sample) with 4-cm^{-1} resolution. The Raman cell was made of two independent compartments connected by a valve: one containing liquid chloroform and the other filled with the dehydrated NaY material (obtained after 12 h of evacuation at 800 K). At time zero, the connection was opened and the zeolite was exposed to gaseous chloroform. Raman spectra were collected every 10 min. In a typical data collection, 100−500 scans were added and normalized at each time. After 6 h, no further change in the Raman spectra was observed, indicating that equilibrium had been reached. The amount of chloroform adsorbed at equilibrium was estimated by gravimetry to be 2.85 ± 0.15 molecules per supercage. A spectrum of liquid chloroform at room temperature was also obtained for comparison.

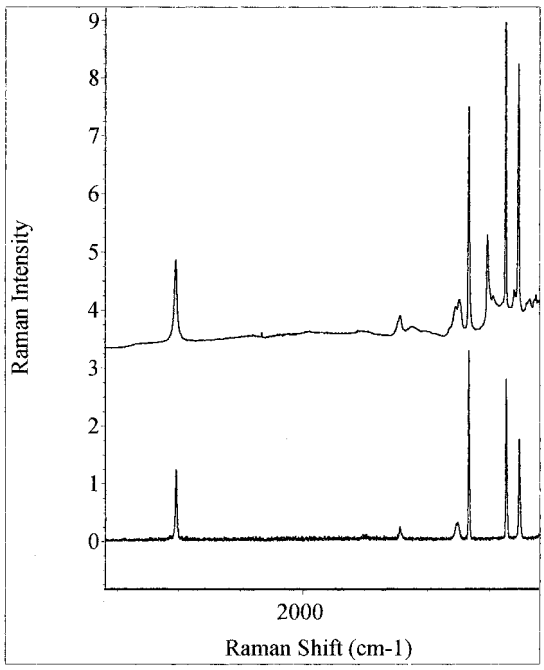

Figure 3. Raman spectra at room temperature of chloroform, run as a liquid (lower spectrum), and of chloroform in NaY zeolite at a loading of ~3 molecules/supercage (upper spectrum).

TABLE 1: Parameters for Short- and Long-Range Interactions

Zeolite−Halocarbon Short-Range Parameters

	ϵ_{ij} (K)	r^*_{ij} (Å)		ϵ_{ij} (K)	r^*_{ij} (Å)
O···C	87.06	3.25	Na···C	13.24	3.69
O···H	90.53	2.70	Na···H	11.41	3.10
O···Cl	181.93	3.43	Na···Cl	212.48	2.90

Zeolite−Halocarbon Long-Range Parameters

atom type	T(Si,Al)	O	Na	C	Cl	H
charge	+2.15	−1.2	+1	−0.102	−0.026	+0.180

TABLE 2: Internal Vibrational Frequencies (cm^{-1}) of Chloroform in Gas and Solid Phases (tw: This Work)

		gas	solid	$CHCl_3$ in NaY	
		IR	INS	INS	Raman
attribution	mode	ref 40	tw	tw	tw
(C−H) stretching	ν_1	3030			3018
(C−Cl) stretching	ν_2	672	663	695 (?)	665
(C−Cl_3) "umbrella" deformation	ν_3	363	365	340	369
(H−C−Cl) bending	ν_4	1219	1218	1246	1231/1211
(C−Cl) stretching	ν_5	760	752	772	775/741
(Cl−C−Cl) bending	ν_6	261	262	264	264

Results

Docking of Chloroform in NaY. The most favorable binding sites for chloroform in NaY were found in the 12-ring

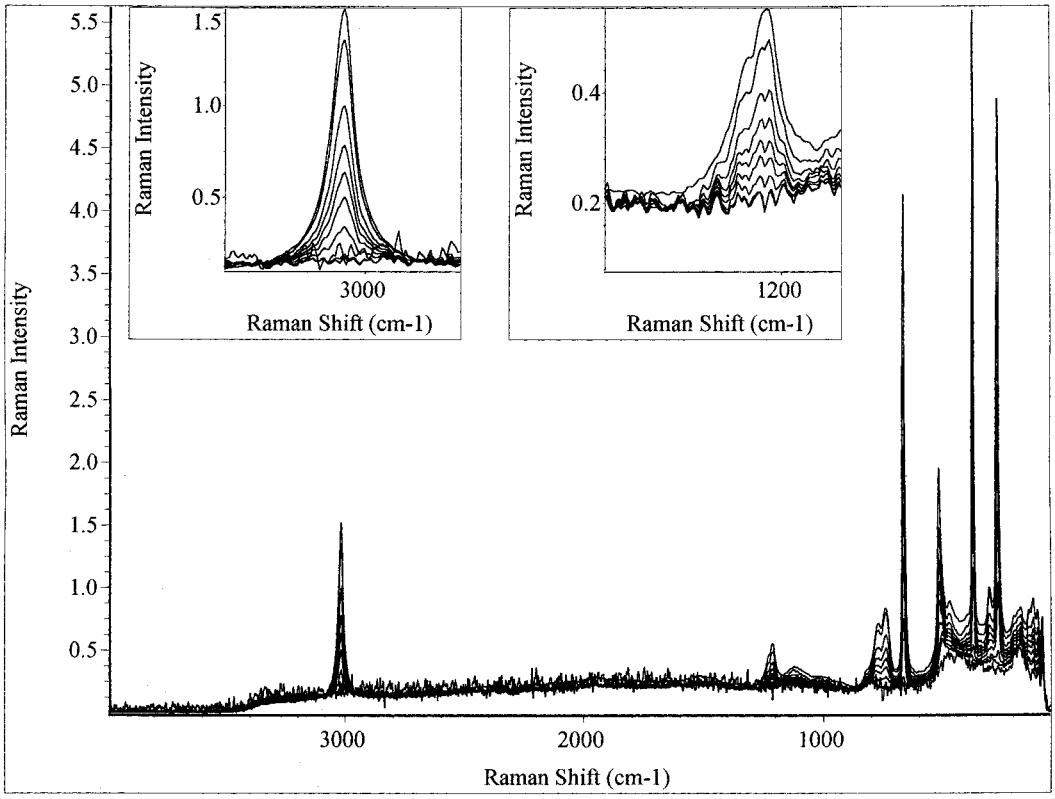

Figure 4. Adsorption of chloroform in NaY zeolite followed by in situ Raman spectroscopy at room temperature.

windows; no binding sites were found close to Na in site II. All favorable binding geometries have broadly similar orientations and binding energies of ~66 kJ/mol. Figure 1b shows a typical geometry. Each chlorine atom is close to at least two framework oxygens with Cl···O distances ranging from 3.5 to 3.8 Å, consistent with van der Waals distances. One of the essential features of the binding geometry is that the C−H bond points toward a framework oxygen, at a typical H···O distance of 2.75 Å. The simulated binding geometry is in close agreement with ref 19 regarding the location of chlorine atoms but differs in terms of the C−H bond orientation. Specifically, the experiment suggests that the C−H bond points toward the center of the supercage (Figure 1a), while our results indicate that it points toward the wall as a result of hydrogen bonding. The authors of ref 19 noted the possibility that the chloroform orientation may be incorrect because the X-ray scattering from the sorbate is dominated by the chlorine atoms, rather than C and H.

Although the binding energy reported above was estimated from 0 K calculations, our computed value is consistent with the experimental heat of adsorption of chloroform in NaY of ~55 kJ/mol at room temperature and the zero-coverage limit.[38] From our docking simulations, the electrostatic contribution arising from the interaction of the dipole moment of $CHCl_3$ with the electric field generated by the zeolite is estimated to be ~25 kJ/mol, the remaining 41 kJ/mol arising from short-range interactions between chloroform and the zeolite. The high contribution of short-range interactions arises because chlorine and oxygen atoms both have high polarizabilities.

Adsorption of chloroform at the SII cation site is not apparent either in the diffraction work or in our simulations. However, Na cations are believed to play a role in determining the orientation of the $CHCl_3$ molecule in the electrostatic field within the supercage since Cl atoms point toward Na cations in site SII according to both the diffraction and simulation work (see Figure 1). In all respects, chloroform adsorption may be considered as a specific adsorption process, owing to the strong contribution of electrostatic interactions in comparison with normal hydrocarbons.

Spectroscopic Results. In the first instance we used INS spectroscopy in order to obtain experimental evidence for hydrogen bonding; INS is uniquely sensitive to vibrational modes involving hydrogen atoms, whereas framework motions give rise to much weaker scattering.[39] The positions of the absorption peaks that were obtained on the solid chloroform sample are in close agreement with the ones already given in the literature; the assignments given in Table 2 are based on previous spectroscopic studies.[40−42] Figure 2 shows the INS spectra of solid chloroform at 15 K (a) and chloroform adsorbed in NaY at 25 K (b), where the spectrum of the dehydrated NaY has been subtracted.

In the following discussion, the vibrational frequencies of gaseous chloroform are considered as a reference for studying shifts upon adsorption in zeolite NaY. The most significant change in the INS spectra upon adsorption of $CHCl_3$ is the broadening and the upward frequency shift by 27 cm^{-1} of ν_4, the H−C−Cl bending mode. The Cl−C−Cl bending mode, ν_6, is virtually unaffected by adsorption, whereas the $C-Cl_3$ deformation mode, ν_3, appears to show a softening for the sorbed molecule. In addition, new framework modes are evident at 463 and 527 cm^{-1}, which derive their enhanced INS intensity from coupling with the adsorbate molecule. This effect is not, of course, removed by the background subtraction. It should also be noted that the INS band intensities are somewhat redistributed for the adsorbate system relative to those in the bulk solid. This is likely to be the result of changes upon adsorption in the H-atom displacements that contribute to the various modes.

In light of the INS results, we used Raman spectroscopy to obtain further evidence for hydrogen bonding between chloro-

form and the framework oxygens. Since Raman spectroscopy is more sensitive, in general, than INS, it offers rapid data collection and the possibility of following, in situ, the coverage dependence of the sorbate vibrations. Figure 3 compares the Raman spectra of liquid chloroform and of the NaY + chloroform sample at a loading of ∼3 molecules per cage at room temperature (without subtraction). In the latter spectrum, the six vibrational fundamentals of chloroform are clearly observed, revealing that the chemical integrity of the chloroform molecules is preserved upon adsorption. In the following, the vibrational frequencies of gaseous chloroform are again considered as a reference for studying the shifts occurring upon adsorption. The two most significant changes are (i) a broadening and a downward frequency shift of the C−H stretching mode ν_1 of 12 cm^{-1}; (ii) a significant broadening and an upward frequency shift of the H−C−Cl bending mode, ν_4, as is observed in the INS spectrum at low loading (∼1 molecule per supercage). Raman spectroscopy reveals that at high loading (∼3 molecules per supercage), this single contribution is replaced by two overlapping peaks, located respectively at 1211 (main peak) and 1231 cm^{-1} (shoulder).

The most significant spectra collected by Raman during in situ adsorption of chloroform are shown in Figure 4. The six internal modes of vibration of chloroform are not apparently shifted as a function of the chloroform coverage. Two additional framework vibrations at 514 and 472 cm^{-1}, whose intensities increase with the overall amount of adsorbed chloroform, were also detected. This finding is consistent with the INS results.

Discussion

Our computer simulations point clearly toward a model in which the H atoms of chloroform molecules adsorbed on a NaY zeolite are involved in hydrogen bonding with the framework oxygens. The information provided by INS and Raman spectroscopies are entirely consistent with this prediction. These techniques reveal that, whatever the temperature (25 K and room temperature) and the coverage, the adsorption of chloroform leads to both a softening of the C−H stretching mode (ν_1) and a hardening of the bending mode (ν_4) involving the H atom; this is characteristic of hydrogen-bonding interactions.[43] In addition, the broadness of the ν_4 peak in INS and the splitting of this vibration in Raman indicate that in a NaY zeolite, the chloroform molecules are likely to be adsorbed at a number of similar sites with slight differences in their energies, a fact that is indeed consistent with our simulations. The apparent differences between the INS and Raman spectra regarding the (C−Cl) stretching and deformation modes (ν_3 and ν_5) may stem from the better resolution of the Raman spectra (thus, for example, resolving a small splitting in ν_5) or may arise from a difference in the temperatures of the measurements or a small dependence of frequency shifts upon coverage.

Several previous studies have pointed to the importance of hydrogen bonding when chloroform interacts with Lewis bases. These include early NMR studies of systems such as chloroform−acetone[44] and IR measurements of chloroform molecules diluted in various polar solvents (acetone, triethylamine, DMSO, and THF).[41,45] With these solvents, the energy of the hydrogen bonds has been estimated to be 10−15 kJ/mol.[44,45] The presence of hydrogen bonding for chloroform molecules adsorbed in faujasite zeolites has also been suggested in a recent IR study.[16]

Conclusion

A large amount of previous work has demonstrated that force-field methods are capable of simulating the structural properties of simple hydrocarbons in zeolite systems. Our work has extended this approach to the more complex situation that is encountered with halocarbon sorbates. There are three contributions to the interaction between adsorbed chloroform and the zeolite host that can be considered as key features of host−guest interactions for systems involving hydrochlorocarbons: (i) there is a substantial contribution arising from the short-range van der Waals forces between chlorine and oxygen, (ii) the electrostatic interaction between chlorine atoms and accessible sodium cations is also important, and (iii) hydrogen bonding plays a significant role and drives the orientation of the sorbate in the zeolite cage. In future publications, we shall show how our force-field simulations can be used to predict thermodynamic properties of chloroform in faujasites and can be extended to other systems of this general class.

Acknowledgment. This work was supported by the U.S. Department of Energy under Grant No. DE-FG03-96ER14672. The work made use of computing facilities supported by the MRL Program of the National Science Foundation under Award No. DMR96-32716. It also benefited from the use of facilities at the Manuel Lujan Jr. Neutron Scattering Center, a National User Facility funded as such by the office of Basic Energy Sciences, U.S. Department of Energy. C.F.M. acknowledges the French Ministère des Affaires Etrangères for a Lavoisier fellowship.

References and Notes

(1) Manzer, L. E. *Science* **1990**, *249*, 31.
(2) Hutchings, G. J.; Heneghan, C. S.; Hudson, I. D.; Taylor, S. H. *Nature* **1996**, *384*, 341. See also: Mukhopadhyay, H.; Moretti, E. C. *Current and Potential Future Industrial Practices for Reducing and Controlling Volatile Organic Compounds*; American Institute of Chemical Engineers, Center for Waste Management: New York, 1993.
(3) Zarchy, A. S.; Maurer, R. T.; Chao, C. C. U.S. Patent 5 453 113, 1994.
(4) Corbin, D. R.; Mahler, B. A. World Patent, W.O. 94/02440, 1994.
(5) Alvarez-Cohen, L.; McCarty, P. L.; Roberts, P. V. *Environ. Sci. Technol.* **1993**, *27*, 2141.
(6) Weber, G.; Bertrand, O.; Fromont, E.; Bourg, S.; Bouvier, F.; Bissinger, D.; Simonot-Grange, M. H. *J. Chim. Phys.* **1996**, *93*, 1412.
(7) Stach, H.; Sigrist, K.; Radeke, K.-H.; Riedel, V. *Chem. Tech.* **1994**, *5*, 278.
(8) Kobayashi, S.; Mizuno, K.; Kushiyama, S.; Aizawa, R.; Koinuma, Y.; Ohuchi, H. *Ind. Eng. Chem. Res.* **1991**, *30*, 2340.
(9) Kawai, T.; Yanagihara, Tsutsumi, K. *Colloid. Polym. Sci.* **1994**, *272*, 1620.
(10) Hannus, I.; Ivanova, I. I.; Tasi, G.; Kiricsi, I.; Nagy, J. B. *Colloids Surf.* **1995**, *A101*, 199.
(11) Cheung, T. T. P. *J. Phys. Chem.* **1992**, *96*, 5505.
(12) Kladnig, W.; Noller, H. *J. Catal.* **1973**, *29*, 385.
(13) Murray, D. K.; Chang, J. W.; Haw, J. F. *J. Am. Chem. Soc.* **1993**, *115*, 4732.
(14) Murray, D. K.; Howard, T.; Goguen, P. W.; Krawietz, Haw, J. F *J. Am. Chem. Soc.* **1994**, *116*, 6354.
(15) Grey, C. P., Corbin, D. R. *J. Chem. Phys.* **1995**, *99*, 16821.
(16) Xie, J.; Huang, M.; Kaliaguine, S. *React. Kinet. Catal. Lett.* **1996**, *58*, 217.
(17) Chintawar, P. S.; Greene, H. L. *J. Catal.* **1997**, *165*, 12.
(18) Gameson, I.; Rayment, T.; Thomas, J. M.; Wright, P. A. *J. Phys. Chem.* **1988**, *92*, 988.
(19) Kazkur, A. Z.; Jones, R. J.; Couves, J. W.; Waller, D.; Catlow, C. R. A.; Thomas, J. M. *J. Phys. Chem. Solids* **1991**, *52*, 1219.
(20) Kazkur, A. Z.; Jones, R. J.; Waller, D.; Catlow, C. R. A.; Thomas, J. M. *J. Phys. Chem.* **1993**, *97*, 426.
(21) Grey, C. P.; Poshni, F. I.; Gualtieri, A. F.; Norby, P.; Hanson, J. C.; Corbin, D. R. *J. Am. Chem. Soc.* **1997**, *119*, 1981.
(22) George, A. R.; Freeman, C. M.; Catlow, C. R. A. *Zeolites* **1996**, *17*, 466.
(23) Freeman, C. M.; Catlow, C. R. A.; Thomas, J. M.; Brode, S. *Chem. Phys. Lett.* **1991**,*186*, 137.
(24) Vitale, G.; Mellot, C. F.; Cheetham. A. K. *J. Phys. Chem.*, **1997**, *B101*, 10518.
(25) Nicholson, D.; Boutin, A.; Pellenq, R. J.-M. *Mol. Simul.* **1996**, *17*, 217.

(26) Yashonath, S.; Thomas, J. M.; Nowak, A. K.; Cheetham, A. K *Nature* **1988**, *331*, 601.
(27) Smit, B.; den Ouden, C. J. J. *J. Phys. Chem.* **1988**, *92*, 7169.
(28) Mellot, C.; Lignières, J. *Mol. Simul.* **1997**, *18*, 349.
(29) Pellenq, R. J. M.; Nicholson, D. *J. Chem. Soc., Faraday Trans.* **1993**, *89*, 2499.
(30) Vitale, G.; Mellot, C. F.; Bull, L. M.; Cheetham, A. K. *J. Phys. Chem.* **1997**, *B101*, 4559.
(31) Ruthven, D. M. *Principles of Adsorption and Adsorption Processes*; Wiley: New York, 1984.
(32) Kramer, G. J.; Farragher, N. P.; van Beest, B. W. H.; van Santen, R. A. *Phys. Rev. B* **1991**, *43*, 5068.
(33) Ghermani, N. E.; Lecomte, C.; Dusausoy, Y. *Phys. Rev. B* **1996**, *53*, 5231.
(34) Ahlrichs, R.; Bär, M.; Häser, M.; Horn, H.; Kölmel, C. *Chem. Phys. Lett.* **1989**, *162*, 165. TURBOMOLE is distributed by MSI, 9685 Scranton Rd., CA 92121-277.
(35) Henson, N. J.; Auerbach, S. M.; Peterson, B. K. *DIZZY Computational Chemistry Program*; Los Alamos National Laboratory, Los Alamos, NM and University of Massachusetts, Amherst, MA, 1994−1998.
(36) Taylor, A. D.; Wood, E. J.; Goldstone, J. A.; Eckert, J. *J. Nucl. Instrum. Methods Phys. Res.* **1984**, *221*, 408.
(37) Sivia, D. S.; Vorderwish, P.; Silver, R. *J. Nucl. Instrum. Methods Phys. Res.* **1990**, *A290*, 492.
(38) Mellot, C. F.; Cheetham, A. K.; Harms, S.; Savitz, S.; Gorte, R. J.; Myers, A. L. Manuscript submitted for publication.
(39) Eckert, J. *Physica* **1986**, *136B*, 150. See also: *Spectroscopic Applications of Inelastic Neutron Scattering*; Eckert, J., Kearley, G. J., , Eds.; *Spectrochim. Acta* **1992**, *48A* (Special Issue).
(40) Herzberg, G. *Infrared and Raman Spectra*; Van Nostrand: Princeton, NJ, 1945.
(41) Devaure, J.; Turrell, G.; Van Huong, P.; Lascombe, J. *J. Chim. Phys.* **1967**, 1064.
(42) Andrews, B.; Anderson, A.; Torrie, B. *Chem. Phys. Lett.* **1984**, *104*, 65.
(43) Novak, A. *Struct. Bonding* **1974**, 18, 177.
(44) Huggins, C. M.; Pimentel, G. C.; Shoolery, J. N. *J. Chem. Phys.* **1955**, *23*, 1244.
(45) Murphy, A. S. N.; Rao, C. N. R. *Appl. Spectrosc. Rev.* **1963**, *2*, 69.